Path Loss Models for Urban Macro Cell Scenario at 3.35, 4.9 and 5.4 GHz

Hang Zheng*, Wei Li†, Lei Tian*, Chongpeng Xu*, Fusheng Huang*, Jianhua Zhang*

*Key Lab of Universal Wireless Communications, Ministry of Education
Beijing University of Posts and Telecommunications, Beijing, China, 100876
Email: hangzheng1990@bupt.edu.cn
† The State Radio Monitoring Center, Beijing, China, 100037
Email: liwei@srrc.org.cn

***Abstract*—In this paper, the channel measurements for 5th generation mobile networks (5G) potential spectrum at 3.35 GHz, 4.9 GHz and 5.4 GHz have been performed in the urban macro cell scenarios in China. The measured cases include line-of-sight (LOS) and non-line-of-sight (NLOS) propagation. After acquiring the channel impulse response from the measurement data, the empirical log-distance path loss models are derived. Free-space and ITU-R models are analysed as references. To explore the relation between path loss and carrier frequency, we revise the proposed path loss models by introducing the frequency dependence coefficient (FDC). Furthermore, when FDC is applied, a more accurate description of path loss differences among three frequencies can be obtained in NLOS case. Measurements can be implemented in more scenarios to acquire optimised channel models in the future.**

I. Introduction

The propagation characteristics are needed to research for IMT-2020 system due to new features for 5G and extended spectrum [1]. ITU-R M.2320 provides a broad view of future technical aspects of terrestrial IMT systems considering the time-frame 2015-2020 and beyond [2]. To meet the demands, new frequency bands should be utilized to provide much more spectrum than available today for LTE systems. IMT-2020 Promotion Group proposed a scheme for IMT spectrum that potential frequency bands below 6 GHz can be researched in short and mid-term until World Radio Conference in 2015 (WRC-15), and frequency bands above 6GHz are long-term targets [3].

Considering about the frequency allocation presently, 3.35 GHz band (3.3 GHz-3.4 GHz), 4.9 GHz band (4.8 GHz-4.99 GHz) and 5.4 GHz band (5.35 GHz-5.47 GHz) are three potential spectrums for 5G mobile communication service. The performance of the wireless mobile communication system is determined by the propagation characteristics of the radio channel. The path loss models are important for network coverage and performance analysis for IMT-2020 system. To provide fundamental theoretical basis for the design, evaluation and actual deployment for future mobile networks, the path loss models at 3.35 GHz, 4.9 GHz and 5.4 GHz should be thoroughly investigated.

In urban scenarios, the wave propagation characteristics are influenced by the density, height and distribution of buildings, etc. Channel measurement in actual scenarios is a direct and effective way to develop the channel model of the specific measured region. Outdoor urban macro cell path loss models for different frequency bands has been covered in the literature. Path loss and delay spread of four frequencies was measured in urban area in [4], but it only measured one frequency that is above 3GHz. Comparison of three empirical path loss models in different scenarios was conducted in [5], and it was found that the ECC-33 model shows the best results in urban environments. As the authors were aimed at comparing empirical models, only 3.5GHz was studied through the measurement. Path loss of 3.5 GHz in urban micro cell scenario was studied in [6] compared to more well-known frequency of 1.9 GHz. However, other frequencies above 3.5 GHz were not discussed. This paper complements the previous work by specifically addressing the urban macro cell scenario and focusing on the 3.35 GHz, 4.9 GHz and 5.4 GHz bands. The path loss models are investigated by field measurements in Xi'an with the aim of developing path loss models which are useful for standardization work and rudimentary planning purposes.

The relation between path loss difference and carrier frequency is also discussed in the paper. It was found that path loss exponent strongly depends on the carrier frequency in [7], and a path loss exponent variation model was proposed in [8]. However, the path loss difference between different frequencies was not studied. In [9], the frequency coefficient is assumed to be 20, which is identical with ITU-R M.2135 [10]. The frequency coefficient is influenced by NLOS environment, which is defined to be 23 in various scenarios in WINNER+ [11]. In this paper, the path loss frequency dependence coefficient is introduced to revise the path loss models.

The rest of the paper is organized as follows. The planform and measurement campaign are described in Section II. After measurement data post processing is explained, results and analysis of path loss models are discussed in Section III. Conclusion of this paper is presented in Section IV.

II. Measurement Campaign

2.1 Measurement Setup

The measurement platform is depicted in Fig. 1. An Agilent E4438C signal generator is used to generate BPSK-modulation signals with a 255-bits-length pseudo-

978-1-4673-6782-0/15/$31.00 ©2015 IEEE

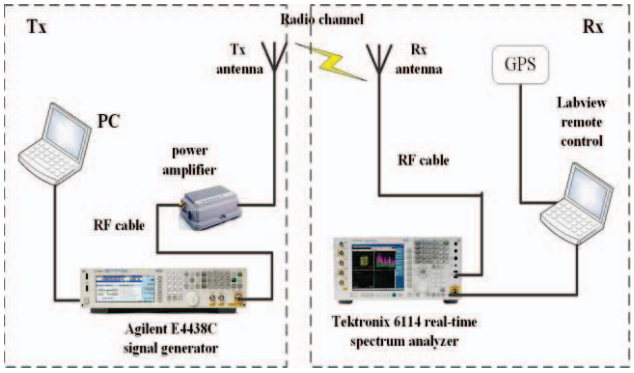

Fig. 1 Measurement platform

random sequence, of which the symbol rate and bandwidth are 30 Msps and 60 MHz, respectively. The power amplifier module follows with an output power of nearly 40 dBm. As we have three frequency bands to measure, three pairs of dipole antennas were prepared, each corresponding to one frequency band. The signals from receiver side (RX) antenna are recorded by Tektronix 6114 real-time spectrum analyzer, which can be controlled by PC with a Labview program to accurately configure the sampling interval and other measurement parameters. A GPS recorder was used to precisely record the measurement location information.

2.2 System Calibration

The Friis transmission equation proposed a basic formula to calculate free-space transmission loss [12]:

$$\frac{P_{rx}}{P_{tx}} = \frac{A_{rx}A_{tz}}{d^2\lambda^2} \quad (1)$$

where P_{tx} and P_{rx} denote transmitted and received power. A_{tx} and A_{rx} denote the effective area of the transmitting and receiving antennas. d is the distance and λ is the wavelength, both in meters. For ideal isotropic antennas, this formula can be simplified and the free-space path loss is defined as follows in dB:

$$PL_{free} = P_{tx} - P_{rx} = 20\log_{10}(d) + 20\log_{10}(f) + 32.45 \quad (2)$$

where f is the frequency in GHz. Considering about the influence of antennas and RF cables, the path loss formula can be revised as:

$$PL = P_{tx} - P_{rx} + G_{tx} + G_{rx} - CL \quad (3)$$

where G_{tx} and G_{rx} denote the calibrated value of transmitter and receiver antenna gain in dBi. CL is the RF cable loss which is calibrated with R&S ZNB-40 Vector Network Analyzer. All the calibration results are utilized in measurement data post processing.

2.3 Measurement Scenarios and Procedures

Extensive measurements of urban macro cell scenario were performed in Xi'an. Xi'an is a typical large Chinese city with compact grid building layout, which is similar to the Manhattan structure.

The aerial map of measurement locations and measurement routes is shown in Fig. 2, in which the star mark shows the location of transmitter and the red lines represent the measurement routes. Measurements were done along different routes and categorized according to LOS and NLOS conditions. In average about 8000 measurement files were sampled within one frequency band measurement at one location. Each measurement file consisted of 10000 samples taken at an interval of 0.25 s. The measurement region coverage is about 500 m from the base station (BS) site.

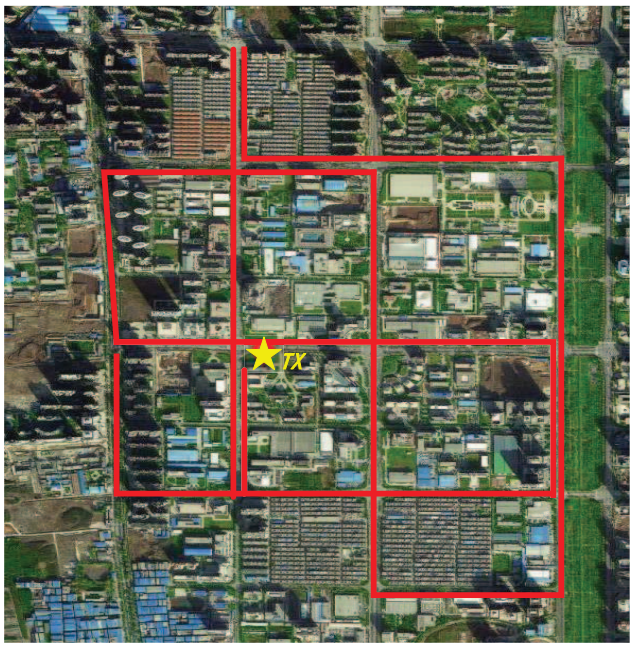

Fig. 2 Measurement routes in Xi'an

Fig. 3 Overview of BS, MS and measurement scenarios

An overview of BS, mobile station (MS) and measurement scenario is shown in Fig. 3. Top left is the BS antenna, which is located in the rooftop of a building fixed with a telescopic mast. Top right is the MS antenna attached to a mast setting up on the top of a van which was used during the measurement. Bottom left and right are the north view and south view of measurement environment from the BS site.

III. Results and Analysis

3.1 Measurement Data Post Processing

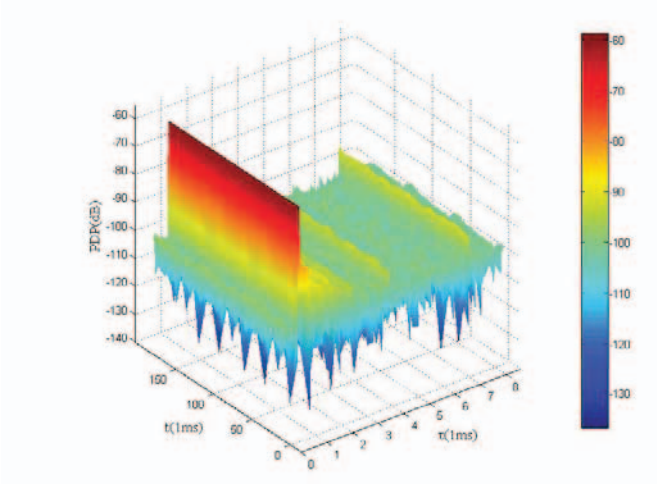

Fig. 4 A typical PDP result at one measurement location

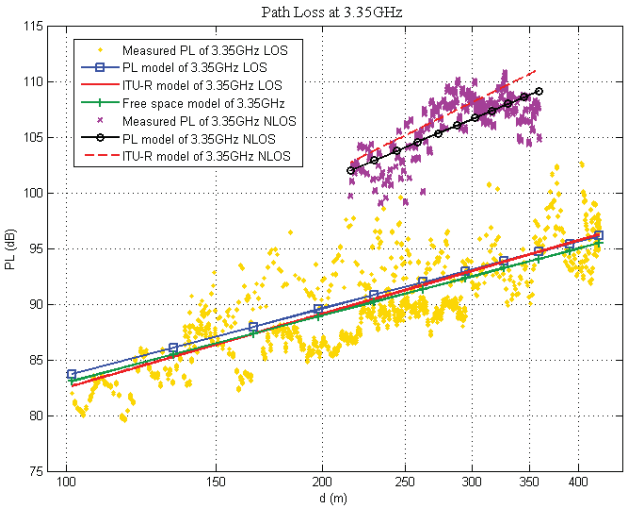

Fig. 5 Path loss results at 3.35 GHz

Measurement data post processing consists of two procedures: 1) obtaining channel impulse response (CIR) from raw data; 2) extracting channel parameters, such as delay, power and angles, etc. In this paper, path loss statistics are analysed for urban macro cell scenarios.

CIRs are obtained by slide correlating the received signal with a copy of transmitter side (Tx) pseudo-random sequence. Power delay profile (PDP) reveals the power strength of received signal and travel time of arrived resolvable multi-paths. A typical PDP result at one measurement location is shown in Fig. 4. Where the τ axis represents the CIR information in delay-domain and the t axis identifies the time-varying characteristics. Multiple paths are observed and the strongest one is brought by LOS propagation whose power intensity is about -58 dB. Others are caused by reflection in the environment, among which the strongest power is 24 dB lower than LOS path. The noise level is about -105 dB and leads to a large dynamic range of about 50 dB.

To separate the noise from the measured multipath components, the dynamic range threshold is set as 15 dB from the noise level for both LOS and NLOS cases. After noise cutting, the measured path loss values are calculated in dB as:

$$PL = -10\log_{10}(\sum_{\tau}|h(\tau)|^2) + G_{tx} + G_{rx} - CL \qquad (4)$$

where $h(\tau)$ is the CIRs which satisfy dynamic range prerequisite, and G_{tx}, G_{rx} and CL are defined in section 2.2. To extract the large-scale propagation characteristics, a linear curve fitting method is used which fits the decibel path loss to the decibel distance with a random variation. The empirical model of log-distance path loss is written as:

$$PL(d) = PL_0 + 10n \cdot \log_{10} d + X_\sigma \qquad (5)$$

where PL_0 represents the intercept, and d is the separation distance between transmitter and receiver expressed in meters, and n denotes the path loss exponent which indicates the rate at which path loss increases with respect to distance. The value of n is dependent on the specific propagation environment, like building density and height, etc. Considering the fact that with the same Tx-Rx distance, the surroundings of the Tx and the Rx in one scenario might be greatly different from those in another scenario, the log-normal shadow fading is modeled by a zero-mean Gaussian random variable X_σ in (5) with standard deviation σ. The values of PL_0 and n are identified by using the least square (LS) method, i.e. the difference between the measured and estimated path loss is minimized in a mean square error sense over a wide range of measurement locations.

3.2 Path Loss Models

Our measurement was implemented in Xi'an as urban macro cell scenario, in which three frequency bands are measured in LOS and NLOS environment. Path loss results at 3.35 GHz are plotted in Fig. 5. For comparison purpose, the path loss models of free-space propagation and ITU-R M.2135 are also depicted in Fig. 5. The frees-pace path loss model is used to predict the received signal strength when the transmitter and receiver have a clear, unobstructed LOS path between them, which would be used as reference for LOS environments only. It can be observed from Fig. 5 that in LOS environment, path loss model of 3.35 GHz closely follows the free-space model. In NLOS environment, path loss results of 3.35 GHz are in the vicinity of corresponding ITU-R model. The LS regression curve lies slightly below ITU-R model with mean difference of 1.1 dB.

Measurement results at 4.9 GHz are shown in Fig. 6. In LOS environment, path loss results at 4.9 GHz appear to be slightly fluctuant, and its path loss model is approximately 5 dB higher than free-space and ITU-R models with a close path loss exponent of 2.07. In NLOS environment, path loss model of 4.9 GHz has an intersection with corresponding ITU-R model, and the maximum difference between them is 1.5 dB.

Measurement results at 5.4 GHz are shown in Fig. 7. In LOS environment, path loss model of 5.4 GHz has a close slope with corresponding ITU-R model of 2.06. Due to larger PL_0, the fitting path loss model has an about 4.5 dB mean difference with ITU-R model. In NLOS environment, the coverage of 5.4 GHz measurement is not as far as 3.35 GHz and 4.9 GHz with a maximum distance of 260m, and path loss results at 5.4 GHz are gathered around ITU-R model. The fitting path loss model is a bit higher than referenced ITU-R curve with a 1.3 dB gap in average.

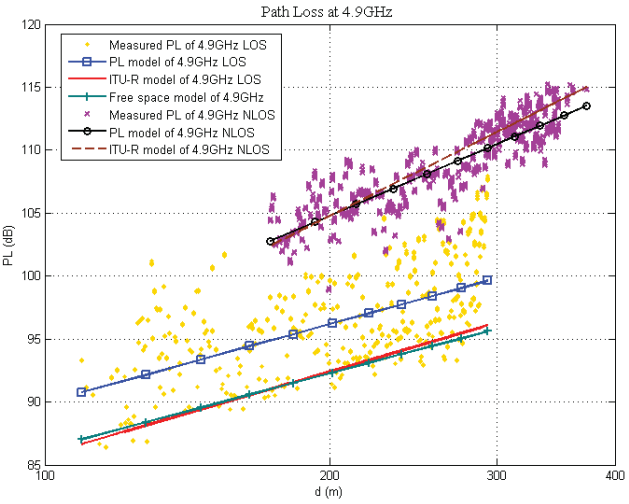

Fig. 6 Path loss results at 4.9 GHz

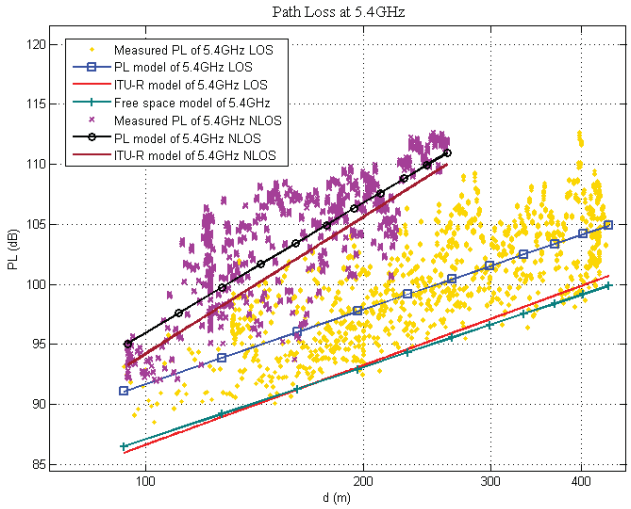

Fig. 7 Path loss results at 5.4 GHz

Summary of parameters for the proposed fitting path loss (PL) models in Xi'an is shown in TABLE I. In LOS environment, the path loss exponents of three frequencies are equal to or a bit larger than 2, which is the path loss exponent of the free-space model. In NLOS environment, the path loss exponents of 3.35 GHz and 4.9 GHz are close, while that of 5.4 GHz tends to be larger. Path loss is increased from 3.35 GHz to 5.4 GHz, and the path loss difference between frequencies is studied as follows in 3.3.

3.3 Revised Models using FDC

In ITU-R M.2135 path loss model, the relation between path loss and carrier frequency is defined as $20\log_{10}(f_c)$ in most cases except for urban micro cell NLOS scenario and when distance d is larger than the break point distance d_{BP} [10]. In LOS environment, path loss is calculated using (2), when $20\log_{10}(f_c)$ can describe the difference of path loss for different carrier frequencies. However, the complexity of NLOS environment makes the influence of carrier frequency on path loss more subtle and the coefficient of $\log_{10}(f_c)$ could be revised [13]. In another widely used channel model WINNER+, frequency dependence is discussed, in which the frequency coefficient is changed to 23 in NLOS

TABLE I
SUMMARY OF PARAMETERS FOR THE FITTING PL MODELS IN XI'AN

	LOS			NLOS		
	n	PL_0	σ	n	PL_0	σ
3.35 GHz	2.00	43.5	2.7	3.23	26.6	1.9
4.9 GHz	2.07	48.6	3.3	3.21	30.8	1.8
5.4 GHz	2.06	50.4	2.8	3.60	24.0	3.2

TABLE II
SUMMARY OF PARAMETERS FOR THE REVISED PL MODELS WITH FDC

	NLOS			
	n	PL_0'	σ	C
4.9 GHz	3.23	30.5	1.8	23.4
5.4 GHz	3.22	32.0	3.2	25.9

TABLE III
PATH LOSS DIFFERENCE BETWEEN FREQUENCIES FOR THREE MODELS

	ΔPL	ΔPL_R	ΔPL_I	ΔPL_W
4.9 GHz	3.9	3.9	3.3	3.8
5.4 GHz	6.2	5.4	4.1	4.8

environment for urban and suburban macro cells and micro cells [11]. Hence, it's necessary to study the frequency dependence of path loss models.

The path loss frequency dependence coefficient (FDC) C is introduced to (5) and the PL model is revised to:

$$PL(d) = PL_0 + 10n \cdot \log_{10} d + X_\sigma + C\log_{10}(\frac{f_c}{f_0}) \quad (6)$$

Where f_c is the carrier frequency and f_0 is the referenced frequency whose path loss characteristics have been measured before. In LOS environment, like free-space propagation formula and other existing models, C is constantly equal to 20. In NLOS environment, PL models of 3.35 GHz are used as references, namely $f_0 = 3.35$, and PL models of 4.9 GHz and 5.4 GHz are retrieved using similarly LS method.

Comparison of path loss models in NLOS environment is shown in Fig. 8. The blue, red and purple solid lines with square markers are the original LS regression curves of 3.35 GHz, 4.9 GHz and 5.4 GHz. The revised PL models of 4.9 GHz and 5.4 GHz are plotted in black and green dash lines with circular markers, and the model parameters are summarised in TABLE II, where:

$$PL_0' = PL_0 + C\log_{10}(\frac{f_c}{f_0}) \quad (7)$$

Let ΔPL denotes the path loss difference between one frequency and the reference frequency 3.35 GHz. The theoretical ΔPL in channel models are calculated by $C\log_{10}(\Delta f)$, where C is the frequency dependence coefficient and Δf is the frequency difference. Path loss differences between 4.9 GHz and 3.35 GHz, 5.4 GHz and 3.35 GHz for three models in dB are listed in TABLE III, where ΔPL is the mean path loss difference of measured results, and ΔPL_R, ΔPL_I, ΔPL_W are the theoretical ΔPL of proposed revised model, ITU-R model and WINNER+ model, respectively. It can be observed from results that ΔPL_R is most accurate in evaluating ΔPL for both 4.9 GHz and 5.4 GHz, while ITU-R model and WINNER+ model underestimate the path loss difference between fre-

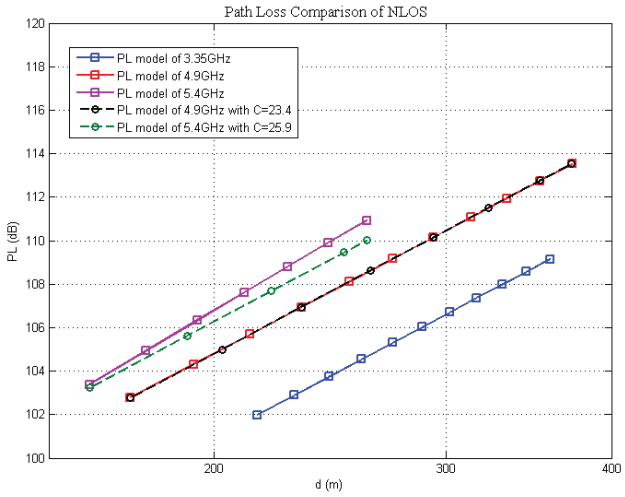

Fig. 8 Comparison of path loss models in NLOS environment

quencies. In overall, introduction of FDC can describe path loss difference between frequencies more precisely with $C = 23.4$ for 4.9 GHz and $C = 25.9$ for 5.4 GHz. More measurements in different scenarios can be implemented to acquire more accurate FDC in the future.

IV. Conclusion

This paper presents the radio channel path loss characteristics of 3.35 GHz, 4.9 GHz and 5.4 GHz in the urban macro cell scenario in Xi'an. Measurement platform was developed and calibration was made in advance. Based on the extensive channel measurements, the empirical log-distance PL models are derived. In LOS case, all PL exponents n are equal or a bit larger than 2. The PL model of 3.35 GHz is consistent with free-space and ITU-R models while that of 4.9 GHz and 5.4 GHz have close slopes and 5 dB gaps. As for NLOS case, the exponent n of three frequencies are 3.23, 3.21 and 3.60. The PL model of 3.35 GHz is slightly below ITU-R model with 1.1 dB gap. For 4.9 GHz, the PL model has an intersection with ITU-R model, and the maximum difference between proposed model and ITU-R model is 1.5 dB. Path loss results at 5.4 GHz are gathered around ITU-R model and the fitting PL model is a bit higher than referenced ITU-R curve with a mean difference of 1.3 dB.

To explore the relation between path loss and carrier frequency, the frequency dependence coefficient (FDC) C is introduced. In LOS case, C is constantly equal to 20. In NLOS case, C is calculated by using results of 3.35 GHz as references. Comparison of the revised model, ITU-R model and WINNER+ model are made that path loss difference can be more exactly described using the revised model with $C = 23.4$ for 4.9 GHz and $C = 25.9$ for 5.4 GHz.

The measurement results are necessary for the technical research and evaluation of 5G planning. Future research could be directed towards implementing measurements in more cities and scenarios to acquire the channel models which can accommodate various environments and to optimise parameters for existing models.

V. Acknowledgments

The research is supported by National Natural Science Foundation of China and project name is "Performance Analysis and Optimization of Relay System in Non-Ideal Channel" with NO. 61171105, National Natural Science Foundation of China and project name is "Theoretical Modeling and Experiment Research of Propagation Channel" with NO. 61322110, National Key Technology Research and Development Program of the Ministry of Science and Technology of China and project name is "Research and Development for Multi-Dimensional Broadband Time-Varying Channel Emulator" with NO. 2012BAF14B01, National 863 Project of the Ministry of Science and Technology and project name is "High efficiency 5G transmission techniques research" with 2014AA01A705. The research is also supported by the State Radio Monitoring Center.

References

[1] Nokia Networks. (2014) 5G use cases and requirements. [Online]. Available: networks.nokia.com/sites/default/files/document/5g_requirements_white_paper.pdf

[2] ITU-R Rec. M.2320, "Future technology trends of terrestrial IMT systems", 2014.

[3] IMT-2020 Promotion Group. (2014) IMT Vision towards 2020 and Beyond. [Online]. Available: www.itu.int/dms_pub/itu-r/oth/0a/06/R0A0600005D0001PDFE.pdf

[4] P. Papazian, "Basic transmission loss and delay spread measurements for frequencies between 430 and 5750 MHz," Antennas and Propagation, IEEE Transactions on, vol. 53, pp. 694-701, 2005.

[5] V. S. Abhayawardhana, et al., "Comparison of empirical propagation path loss models for fixed wireless access systems," in Vehicular Technology Conference, 2005. VTC 2005-Spring. 2005 IEEE 61st, 2005, pp. 73-77 Vol. 1.

[6] I. Rodriguez, et al., "Path loss validation for urban micro cell scenarios at 3.5 GHz compared to 1.9 GHz," in Global Communications Conference (GLOBECOM), 2013 IEEE, 2013, pp. 3942-3947.

[7] D. Cassioli, et al., "The role of path loss on the selection of the operating bands of UWB systems," in Personal, Indoor and Mobile Radio Communications, 2004. PIMRC 2004. 15th IEEE International Symposium on, 2004, pp. 2787-2791 Vol.4.

[8] C. Jinwon, et al., "Frequency-Dependent UWB Channel Characteristics in Office Environments," Vehicular Technology, IEEE Transactions on, vol. 58, pp. 3102-3111, 2009.

[9] S. Aerts, et al., "Empirical path-loss model in train car," in Antennas and Propagation (EuCAP), 2013 7th European Conference on, 2013, pp. 3777-3780.

[10] ITU-R Rec. M.2135, "Guidelines for evaluation of radio interface technologies for IMT-Advanced", 2009.

[11] P. Kyösti, et al., "IST-4-027756 WINNER II D1.1.2 v1.2 WINNER II channel models," In: Journalism Practice, vol. 1, pp. 322--338, 2008.

[12] H. T. Friis, "A note on a simple transmission formula," proc. IRE, vol. 34, pp. 254-256, 1946.

[13] J. Zhang, et al., "Propagation characteristics of wideband MIMO channel in urban micro-and macrocells," in Personal, Indoor and Mobile Radio Communications, 2008. PIMRC 2008. IEEE 19th International Symposium on, 2008, pp. 1-6.